

Heterogenization of manganese porphyrin *via* hydrogen bond in zeolite imidazolate framework-8 matrix, a host–guest interaction, as catalytic system for olefin epoxidation

Mojtaba Bagherzadeh* and Elnaz Mesbahi

Chemistry Department, Sharif University of Technology, P.O. Box 11155-3615, Tehran, Iran

Received 17 April 2018

Accepted 2 July 2018

ABSTRACT: A heterogenized *meso*-tetrakis(2,3-dihydroxyphenyl)porphyrinatomanganese(III) acetate at zeolite imidazolate framework-8 (T(2,3-OHP)PorMn@ZIF-8) is investigated for the catalytic olefin epoxidation reactions at room temperature. Heterogenization is accomplished through a non-classical hydrogen bond proposed between T(2,3-OHP)PorMn bearing O–H groups and C–H of the 2-methylimidazolate linkers in the ZIF-8 structure. The aforementioned compound is characterized by X-ray powder diffraction (XRD), atomic absorption spectroscopy (AAS), nitrogen adsorption–desorption, FT-IR spectroscopy, field emission scanning electron microscopy (FE-SEM), transmission electron microscopy (TEM) and Raman spectroscopy. The catalytic system with rather high potential of reusability is proposed as a fairly efficient epoxidation catalyst compared to reports in homogeneous media.

KEYWORDS: manganese porphyrin, Zeolite Imidazolate Framework-8, non-classical hydrogen bonding, catalytic epoxidation.

INTRODUCTION

Mimicking catalytic function of biological systems including cytochrome-P450, hemoglobin, peroxidase and other oxidative enzymes has always been one of the most interesting targets for scientific researchers [1–7]. Metalloporphyrins have been extensively considered as proper models of enzymes in olefin epoxidations [8–14]. To the best of our knowledge the catalytic activity and stability of metalloporphyrins are influenced by various electronic and steric properties [15, 16]. Recently more attention has been paid to the importance of some interactions such as hydrogen bonds as a dominant factor playing a role in the active site of natural enzymes [17]. A category of carbon–oxygen hydrogen bonding (CH...O) differing from the previously well-known classic type [19] has been documented in biological structures during the last four decades [18]. Aliphatic carbon atoms are

capable of forming such non-classical weak hydrogen bonds [20, 21]. There are some reports in literature documenting existence of the aforementioned category of hydrogen bonds in metalloporphyrin catalytic homogeneous systems [22]. Unusual co-catalytic activity of 2,6-dimethylpyridine in the presence of *meso*-tetrakis(pentafluorophenyl) porphyrinatomanganese(III) acetate (MnTPFP(OAc)) is reported to arise from hydrogen bonding between the *ortho*-C–F moieties of Mn(Por) and the *ortho* methyls on pyridine [23, 24]. The importance of hydrogen bond presence is also evidenced based on the higher activity of manganese porphyrins with hydroxy or methoxy groups at the 2 and 3 positions of the phenyls on the *meso*-substituted porphyrins [25, 26]. Moreover, it has been revealed that *meso*-tetrakis(2,3-dihydroxyphenyl)porphyrinatomanganese(III) acetate performs as a preferable epoxidation catalyst in the presence of 2-methylimidazole in homogeneous media, although it still suffers from lack of recyclability [27]. To overcome this problem, heterogenization of such systems through encapsulation in the cages of the

*Correspondence to Mojtaba Bagherzadeh, email bagherzadeh@sharif.edu.

porous materials such as metal organic frameworks (MOFs) with their favorable properties would help [28–32]. Zeolite imidazolate framework-8 (ZIF-8) is a MOF composed of tetrahedrally-coordinated Zn ions connected by 2-methylimidazolate linkers with external surfaces having hydrophilic properties [33–36]. Its six-membered ring pore windows are narrow enough to prevent the exit of the stuck metalloporphyrins. It is worth mentioning that the existence of a functional group with the ability to produce hydrogen bonds on the porphyrin compound is essential for the encapsulation process [37].

In this work, Mn(por) bearing OH substituents in the *ortho* and *meta* positions of the phenyl groups is heterogenized in a zeolite imidazolate framework (ZIF-8) matrix *via* host–guest interaction (Fig. 1). The OH groups are capable of producing non-classical hydrogen bond with the aliphatic C–H on the 2-methylimidazolate parts of the matrix in the periphery of the porphyrin. Olefin epoxidation in the presence of the heterogenized metalloporphyrin and tetra-*n*-butylammonium hydrogen monopersulfate as oxidant has been examined. It seems that combination of T (2,3-OHP)PorMnOAc with ZIF-8 (T(2,3-OHP)PorMn@ZIF-8) brings about a desirable oxidation catalyst for cyclooctene and cyclohexene, overcoming the reusability problem.

RESULTS AND DISCUSSION

Characterization of T (2,3-OHP)PorMn@ZIF-8

In order to characterize the catalyst structure, the XRD patterns of MnPor@ZIF-8 and ZIF-8 are measured (Fig. 2 and S1). The XRD patterns of both compounds show highly crystalline structures consistent with previous literature reports (Fig. 2) [36, 38]. The similar pattern of characteristic peaks for MnPor@ZIF-8 with a negligible decrease in the intensities indicates that the crystalline structure of ZIF-8 is likely to be retained without significant changes; however, it is influenced by the host–guest interaction.

The formation of such structures was confirmed by the FT-IR technique as well (Fig. 3 and S2) [39]. The characteristic band of ZIF-8 structure relating to Zn–N stretching at 421 cm^{-1} is clearly observed [38, 40]. A very slight shift in the band location around 2931 cm^{-1} which is ascribed to the aliphatic C–H stretch of 2-methylimidazole [41–43] could be occurred as a result of a weak hydrogen bond between C–H of 2-methylimidazole and the porphyrin bearing OH groups.

The amount of T(2,3-OHP)PorMn loaded as determined by atomic absorption spectroscopy was 3.1 mg/g . It is noteworthy that the loading process of

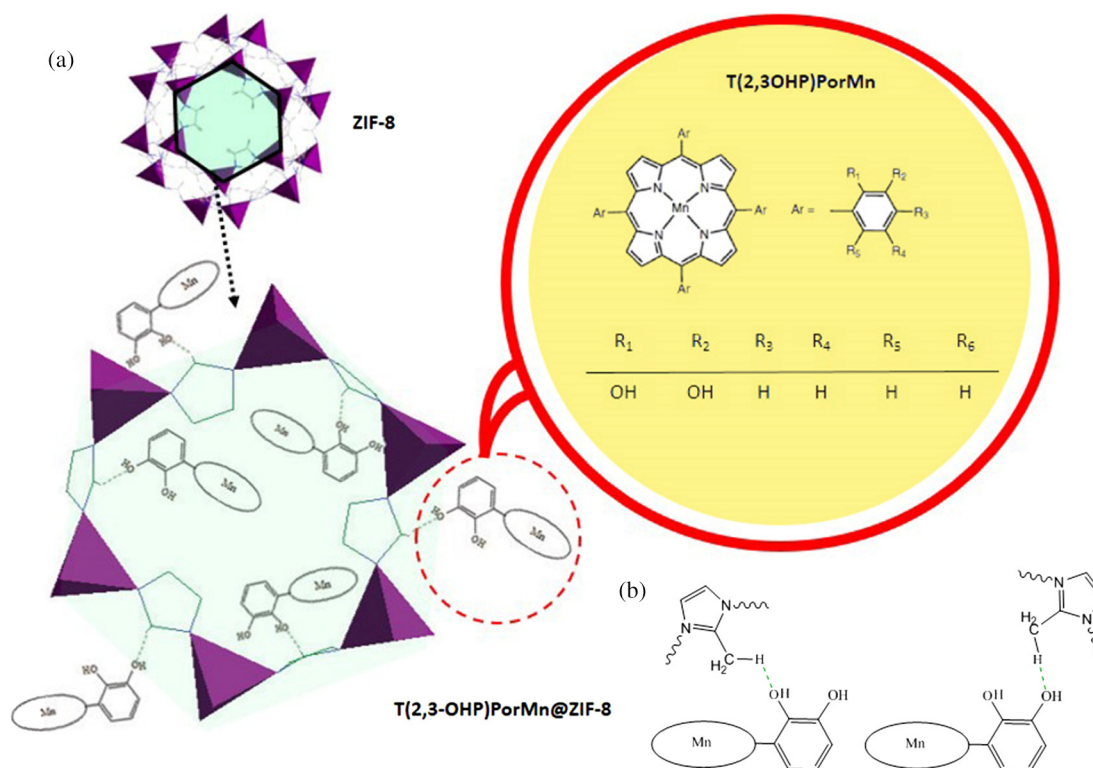


Fig. 1. Schematic structure of (a) T(2,3-OHP)PorMn@ZIF-8 and the moieties prone to hydrogen bonding formation (b) probable hydrogen bond orientation between hydroxy groups of phenyl rings in the effective isomer of T(2,3-OHP)PorMnOAc and 2-methylimidazolate linkers in ZIF-8

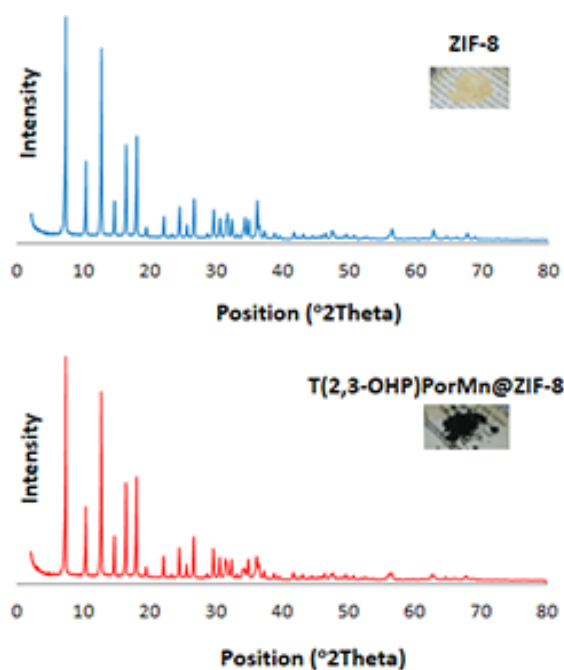


Fig. 2. PXRD pattern of ZIF-8 (blue) and T (2,3-OHP)PorMn@ZIF-8 (red)

T(2,3-OHP)PorMn at ZIF-8 was accompanied by a change in color from cream to gray (Fig. 2). The surface area and pore volume of T(2,3-OHP)PorMn@ZIF-8 has been surveyed through the nitrogen adsorption-desorption method (Fig. S3). As shown in Fig. 4, a type I isotherm is obviously obtained through this investigation with concern to the ones reported by IUPAC [44]. The surface area of BET (Brunauer–Emmett–Teller) and pore volume of T(2,3-OHP)PorMn@ZIF-8 gained $104.19 \text{ m}^2 \cdot \text{g}^{-1}$ and $0.1187 \text{ cm}^3 \cdot \text{g}^{-1}$ respectively (Table 1). A slight increase in the surface area and pore volume of

T(2,3-OHP)PorMn@ZIF-8 compared to that of ZIF-8 may suggest that the host–guest interactions occur mostly on the outer surface of ZIF-8 [45]. In addition, the swing of the imidazolate moieties in ZIF-8 would likely be involved in order to have an appropriate orientation and so the facility of participating in interaction with hydroxyl groups prone to hydrogen bonding [46].

In order to gain more insight into the presence of such interactions, Raman spectra of ZIF-8 and T(2,3-OHP)PorMn@ZIF-8 were compared (Fig. 5). The peak appearing around 1460 cm^{-1} is related to the C–H bonding of the methyl group in the 2-methylimidazolate linkers of ZIF-8 [46]. Whenever any kind of hydrogen bonding takes place, it could affect the appearance of the peak mentioned above and thus shift it slightly. Hence, considering the clear broadening and the slight shift, such an interaction may occur between the OH group moieties on the periphery of the porphyrin and the 2-methylimidazolate in the ZIF-8 structure (Fig. 1). Note that the presence of this unusual kind of hydrogen bonding has already been documented in homogeneous media [25, 27].

The morphology of T(2,3-OHP)PorMn@ZIF-8 has been investigated through field-emission scanning electron microscopy (FE-SEM) and high resolution transmission electron microscopy (HR-TEM) (Fig. 6). It seems that the sample particles are highly eager to aggregate, as shown in the figure. The particular honeycomb of the ZIF-8 structure is also observed [36, 38].

Catalytic epoxidation reaction

Epoxidation of various olefins was investigated in the presence of the heterogenized manganese porphyrin (T(2,3-OHP)PorMn@ZIF-8) in a mixture of CH_2Cl_2 and methanol (in a ratio of 5:1). Tetra-*n*-butylammonium

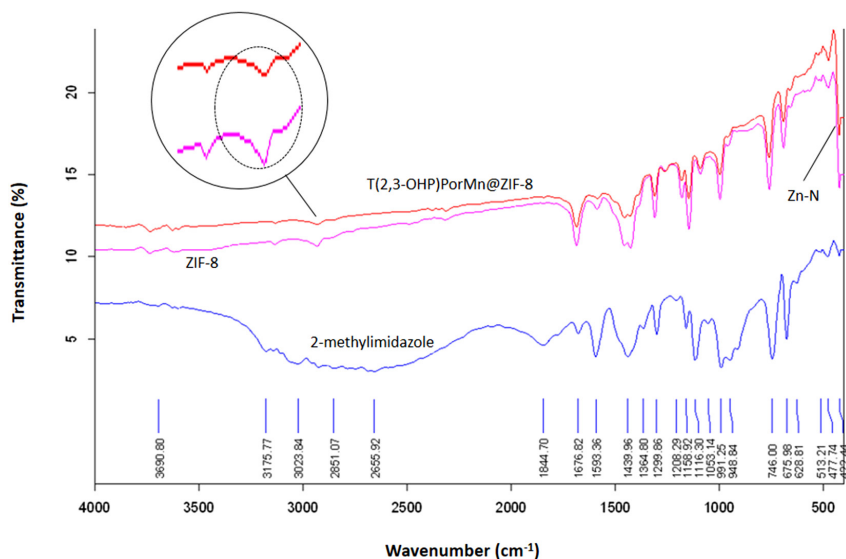


Fig. 3. FT-IR spectra of 2-methylimidazole (blue), ZIF-8 (purple) and T (2,3-OHP)PorMn@ZIF-8 (red)

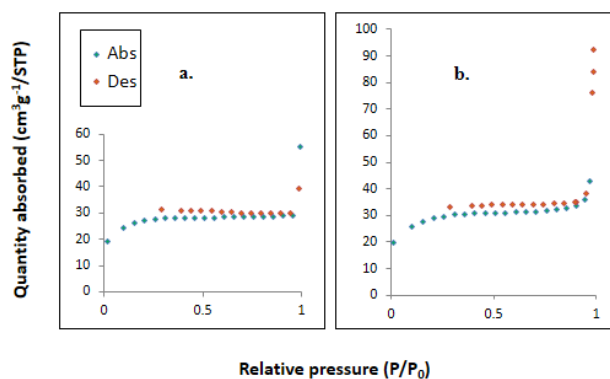


Fig. 4. Representative N_2 adsorption and desorption isotherms of (a) ZIF-8 and (b) T(2,3-OHP)PorMn@ZIF-8

Table 1. Textural properties, $a_{s,BET}$ (BET surface area) and V_p (pore volume)

Sample	$a_{s,BET}$ ($\text{m}^2 \cdot \text{g}^{-1}$)	V_p ($\text{cm}^3 \cdot \text{g}^{-1}$)
ZIF-8	97.325	0.049182
T(2,3-OHP)PorMn@ZIF-8	104.19	0.1187

hydrogen monopersulfate ($n\text{-Bu}_4\text{NHSO}_5$) was used as an oxidant in all the reactions. The ratio of the reactants, catalyst and oxidant concentrations and the reaction time were optimized (Figs 7 and 8). The reactions were all carried out at room temperature and the results obtained through injection into GC after stirring for 18 h. The conversion percentage for various alkenes and selectivity to their corresponding epoxides are presented in Table 2. According to the results shown in Table 2, the greatest amount of conversion is obtained for cyclooctene and cyclohexene. The lower selectivity in the case of cyclohexene compared to cyclooctene is due to the formation of other oxidation products rather than epoxide (entries 1 and 2). Among styrene derivatives, the more electron rich the double bond is, the

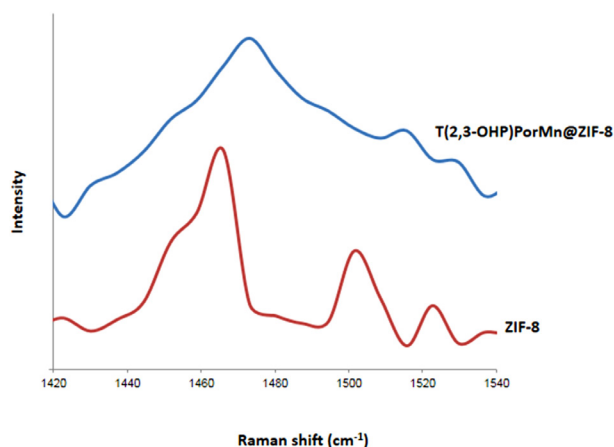


Fig. 5. Raman spectrum of ZIF-8 (red) and T (2,3-OHP) PorMn@ZIF-8 (blue)

greater conversion percentage is achieved (entries 3–6). Moreover, the greater amount of conversion obtained for 4-methoxystyrene in comparison to the analogue species might take place as a result of a more readily entrance or access to the active sites of the catalyst in the hydrophilic moieties. It seems that the active sites of the catalyst are inaccessible in the case of the bulky substrates such as 1-octene, *cis*-stilbene and *trans*-stilbene considering the low conversion and selectivity (entries 7–9).

In order to survey the reusability of our catalyst, it was separated, washed thoroughly with ethanol and dried after centrifuging the reaction mixture at the end of the reaction time. The catalyst was utilized for the next run after preparation as mentioned above. It was revealed that T(2,3-OHP)PorMn@ZIF-8 could be used in six subsequent runs without a considerable decrease in its performance (Fig. 9). The XRD pattern of T (2,3-OHP) PorMn@ZIF-8 after usage in 7 runs seems to be altered compared to those represented in Fig. 2 and indicates a change in the catalyst structure (Fig. 10).

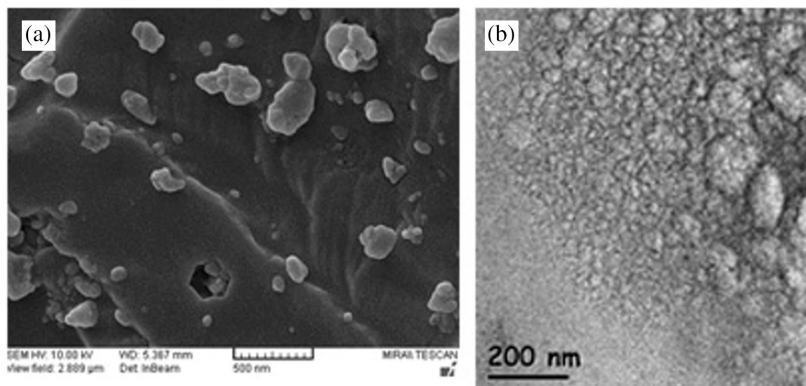
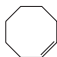
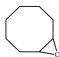
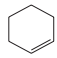
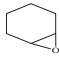
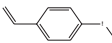
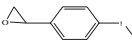
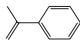
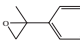
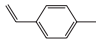
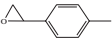
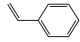
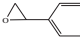
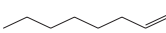
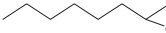
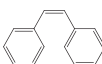
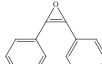
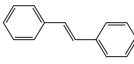
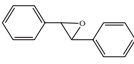


Fig. 6. (a) FESEM of T(2,3-OHP)PorMn@ZIF-8 with the scale bar of 500 nm; (b) HRTEM of T(2,3-OHP)PorMn@ZIF-8

Table 2. Conversion percentage and selectivity to corresponding epoxide of various alkenes in epoxidation reaction

Entry	Substrate	Product	Conversion %	Selectivity to epoxide %
1			87	98
2			97	52
3			70	50
4			55	36
5			24	29
6			28	89
7			11	>99
8			7	43 (21)
9			31	77 (19)

Substrate (0.2 mmol), $n\text{-Bu}_4\text{NH}_5\text{O}_5$ (0.4 mmol), catalyst (3×10^{-4} mmol), CH_2Cl_2 /methanol (5:1), room temperature, 18 h, internal standard method was used.

Comparison of analogue homogenous and heterogeneous media

To compare the performance of T(2,3-OHP)PorMn@ZIF-8 with various analogues reported in literature, the results and conditions of cyclooctene epoxidation in the presence of diverse homogenous and heterogeneous catalytic media is presented in Table 3 [25, 27, 37]. In homogeneous media, the cooperating interplay of hydrogen bonding gives rise to higher conversions in the case of T(2,3-OHP)PorMn/2-methylimidazole and T(2,3-OHP)PorMn/acetate compared to the cases showing a lack of such interaction (entry 2,4 and 3,5).

Note that the idea of heterogenization of T(2,3-OHP)PorMn by the usage of such interactions with 2-methylimidazolate linkers of ZIF-8 (Por-O...HMe-Im, Fig. 1) improved reusability in addition to the increase in conversions. To our surprise, T(4-OHP)PorMn@ZIF-8 showed an impressive increase in conversions compared to the T(4-OHP)PorMn/acetate suffering from lack of such hydrogen bonding in homogeneous media [25]. Thus, T(2,3-OHP)PorMn@ZIF-8 could be considered as a reusable catalyst with the ability to convert cyclooctene to the epoxide (entries 6, 5). The kinetic profile of T(4-OHP)PorMn@ZIF-8 and T(2,3-OHP)PorMn@ZIF-8 in the cyclooctene epoxidation is represented in Fig. 11. An enhancement in the reaction rate is revealed for cyclooctene epoxidation in

the presence of T(4-OHP)PorMn@ZIF-8, which is in agreement with its higher BET surface area (Table S1).

EXPERIMENTAL

Materials

T(2,3-OHP)PorMnOAc and T(4-OHP)PorMnOAc were synthesized based on the porphyrin demethylation method of James [47] starting from 5,10,15,20-tetrakis-(2,3-dimethoxyphenyl)porphyrinatomanganese(III) acetate (T(2,3-OMeP)PorMnOAc) and 5,10,15,20-tetrakis(4-methoxyphenyl)porphyrinatomanganese(III) acetate (T(4-OMeP)PorMnOAc). The corresponding free-base porphyrins were prepared by the Lindsey method [48] and metallated by $\text{Mn}(\text{OAc})_2 \cdot 4\text{H}_2\text{O}$ according to the Adler method [49]. In the end, purification of aforementioned porphyrins with some modification in James' method brought about demethylation and conversion into porphyrins bearing hydroxyl groups. The green mixture containing BBr_3 in CH_2Cl_2 was exposed to heat up to 50°C so that the extra acid not utilized in the reaction and the solvent were evaporated [25].

T(2,3-OHP)PorMn@ZIF-8 and T(4-OHP)PorMn@ZIF-8 were prepared through the template-directed strategy method. 2-Methylimidazolate (0.33 mmol) and $\text{Zn}(\text{NO}_3)_2$ (0.28 mmol) were mixed with manganese porphyrin (0.02 mmol) in DMF (10 ml) and transferred

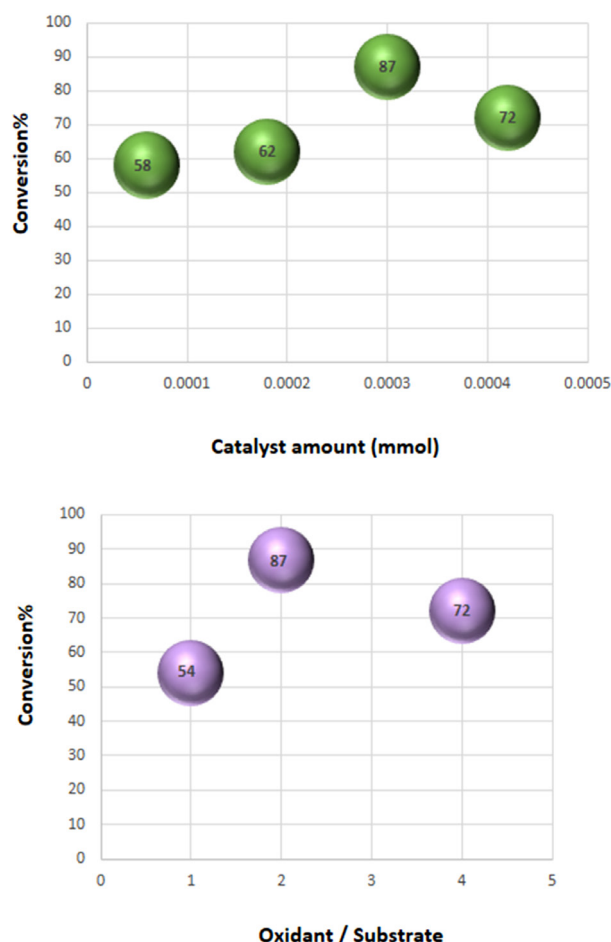


Fig. 7. Optimization of T(2,3-OHP)PorMn@ZIF-8 (green) and $n\text{-Bu}_4\text{NHSO}_5$ (purple) in cyclooctene epoxidation at room temperature, in the mixture of CH_2Cl_2 /methanol (5:1)

into Teflon-lined Parr pressure vessels. The Teflon liners were placed in autoclaves, and heated to 408 K for 36 h [37].

$n\text{-Bu}_4\text{NHSO}_5$, which is the corresponding soluble salt of oxone (the commercial triple potassium salt insoluble in organic solvents), was prepared by a previous method [50].

All other chemical substances were purchased from the Merck, Fluka and Alfa Aesar companies.

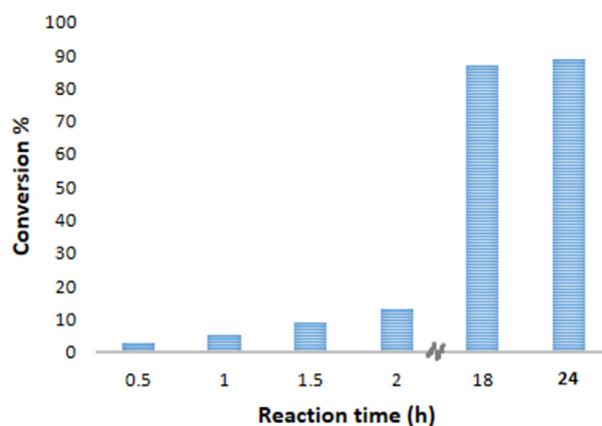


Fig. 8. Conversion percentage of cyclooctene vs. reaction time in the presence of T(2,3-OHP)PorMn@ZIF-8 at room temperature, in the mixture of CH_2Cl_2 /methanol (5:1)

Instrumentation

Diverse instruments were employed to characterize the prepared catalyst. X-ray diffraction (XRD) patterns were obtained by XPERT-PRO diffractometer system (MPD PANalytical Company) using a $\text{Cu K}\alpha$ radiation source (the scan range (2θ) was from 2° to 80°). Nitrogen adsorption-desorption measurements were performed on a Tri Star II surface area and porosity analyzer (Micromeritics). FT-IR spectra were gained through an ABB Bomem MB-100 FT-IR spectrophotometer utilizing KBr disks at room temperature. Raman spectra were recorded on a Rigaku micro Raman spectrometer with a HeNe red laser (1064 nm) and 490 mW laser power (exposure time: 3000 ms). The amount of manganese was determined by a Shimadzu (AA680) atomic absorption/ flame emission spectrometer utilizing air and acetylene. Field emission scanning electron microscopy (FE-SEM) was obtained using a TESCAN MIRA II field-emission scanning electron microscope. Transmission electron microscopy (TEM) was performed on a JEM-2100F (JEOL) microscope operating at 200 kV. Gas chromatographic (GC) analyses were carried out on an Agilent Technologies 6890 N, 19019 J-413 HP-5, capillary $60\text{ m} \times 250\text{ }\mu\text{m} \times 1\text{ }\mu\text{m}$.

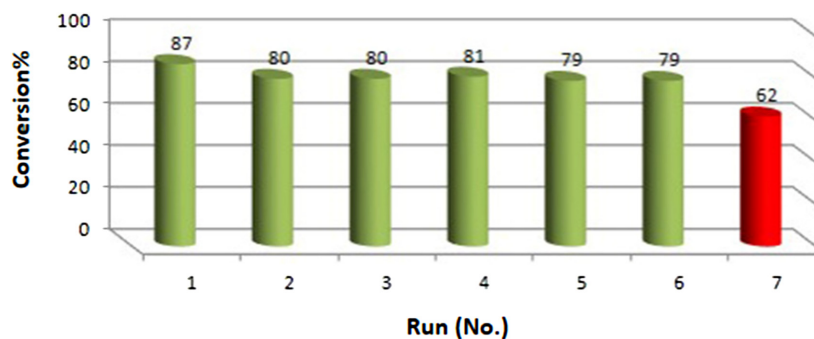


Fig. 9. Profile of cyclooctene conversion % obtained in each run

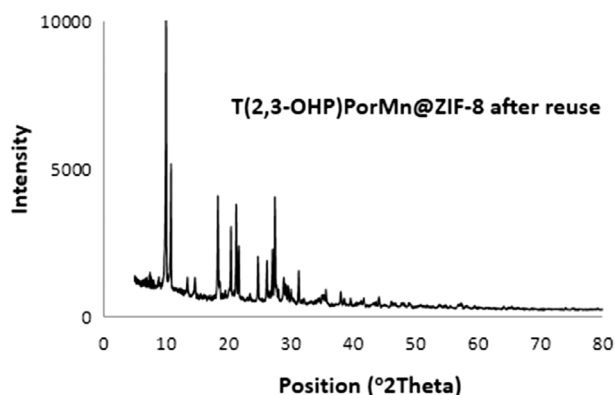


Fig. 10. PXRD pattern of T(2,3-OHP)PorMn@ZIF-8 after usage in 7 runs

Epoxidation reactions

Epoxidation of olefins was investigated in the presence of $n\text{-Bu}_4\text{NHSO}_5$ and MnPor@ZIF-8. The reactions were all carried out in the optimized medium (CH_2Cl_2 and methanol, 5:1) at room temperature. The following molar ratios were used: substrate (0.2 mmol), n -octane (0.12 mmol) as the internal standard, catalyst (3×10^{-4} mmol) and $n\text{-Bu}_4\text{NHSO}_5$ (0.4 mmol). The reactions proceeded in a closed system with stirring for 18 h. The reaction solution (0.2 μL) was injected into the GC system after separation of the catalyst by centrifugation. For reusability studies, the catalyst was washed thoroughly with ethanol and then prepared for usage in the next run.

Table 3. Epoxidation of cyclooctene in distinct catalytic systems

Entry	Catalyst	Conditions	Conversion %
1	T(2,3-OHP)PorMn@ZIF-8	Heterogeneous CH_2Cl_2 /methanol $n\text{-Bu}_4\text{NHSO}_5$ room temperature ^a , 18 h	87
2	T(2,3-OHP)PorMnOAc	Homogeneous CH_2Cl_2 /methanol 2-methylimidazole $n\text{-Bu}_4\text{NHSO}_5$ room temperature, 10 h (24 h) [27]	67
3	T(2,3-OHP)PorMnOAc	Homogeneous CH_2Cl_2 /methanol imidazole $n\text{-Bu}_4\text{NHSO}_5$ room temperature, 10 h [27]	26
4	T(2,3-OHP)PorMnOAc	Homogeneous CH_2Cl_2 /methanol Tetra- n -butylammonium acetate $n\text{-Bu}_4\text{NHSO}_5$ room temperature, 10 h [25]	75
5	T(4-OHP)PorMnOAc	Homogeneous CH_2Cl_2 /methanol Tetra- n -butylammonium acetate $n\text{-Bu}_4\text{NHSO}_5$ room temperature, 10 h [25]	38
6	T(4-OHP)PorMn@ZIF-8	Heterogeneous CH_2Cl_2 /methanol $n\text{-Bu}_4\text{NHSO}_5$ room temperature, 18 h	89
7	Mn-TAPP@ZIF-8	Heterogeneous Acetonitrile TBHP 80 °C, 24 h [37]	62
8	ZIF-8	Heterogeneous CH_2Cl_2 /methanol $n\text{-Bu}_4\text{NHSO}_5$ room temperature, 18 h	39
9	no catalyst	CH_2Cl_2 /methanol $n\text{-Bu}_4\text{NHSO}_5$ room temperature, 18 h	10

No significant difference was observed in results in the presence of imidazole.

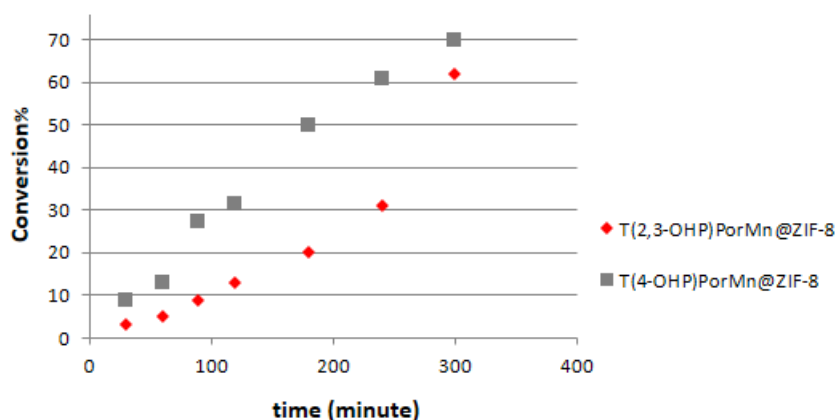


Fig. 11. Kinetic profile of T (2,3-OHP)PorMn@ZIF-8 (red) and T (4-OHP)PorMn@ZIF-8 (gray) in cyclooctene epoxidation reaction

CONCLUSIONS

T(2,3-OHP)PorMn@ZIF-8 and T(4-OHP)PorMn@ZIF-8 were synthesized *via* the hydrogen bond direct approach. The cooperating interplay of a kind of non-classical weak hydrogen bonding has allowed our catalytic system to possess the advantage of heterogeneous catalysts adjoined to analogue homogeneous ones. This is supported by fairly good reusability and also enhanced catalytic efficiency of the catalyst presented. T(2,3-OHP)PorMn@ZIF-8 was consecutively reused five times without significant loss of activity in the cyclooctene epoxidation reaction. Moreover, operating under mild conditions could be considered as another attractive feature of the aforementioned catalytic compound in this work.

Acknowledgments

The support of this work by Research Council of Sharif University of Technology is appreciated.

Supporting information

Figures S1–S3 and Table S1 are given in the supplementary material. This material is available free of charge *via* the Internet at <http://www.worldscinet.com/jpp/jpp.shtml>.

REFERENCES

- Mansuy D. *Comptes Rendus Chim.* 2007; **10**: 392–413.
- Larsen RW, Wojtas L, Perman J, Musselman RL, Zaworotko MJ and Vetromile CM. *J. Am. Chem. Soc.* 2011; **133**: 10356–10359.
- Nam W. *Acc. Chem. Res.* 2007; **40**: 522–531.
- Mansuy D. *Coord. Chem. Rev.* 1993; **125**: 129–141.
- De Montellano PRO, (Ed.). *Cytochrome P450: Structure, Mechanism, and Biochemistry*, Kluwer Academic/Plenum Publishers: New York, 2005.
- Bertini I, Gray HB, Lippard SJ and Valentine JS. *Bioinorganic Chemistry*, University Science Books: Mill Valley, CA, 1994.
- Alemohammad T, Rayati S and Safari N. *J. Porphyrins Phthalocyanines* 2015; **19**: 1279–1283.
- Collman JP, Zhang X, Lee VJ, Uffelman ES and Brauman JI. *Science* 1993; **261**: 1404–1411.
- Dolphin D, Traylor TG and Xie LY. *Acc. Chem. Res.* 1997; **30**: 251–259.
- Groves JT and Nemo TE. *J. Am. Chem. Soc.* 1983; **105**: 5786–5791.
- Rose E, Quelquejeu M, Pandian RP, Leca-Nawrocka A, Vilar A, Ricart G, Collman JP, Wang Z and Straumanis A. *Polyhedron* 2000; **19**: 581–586.
- Bagherzadeh M and Mortazavi-Manesh A. *RSC Adv.* 2016; **6**: 41551–41560.
- Omagari T, Suzuki A, Akita M and Yoshizawa M. *J. Am. Chem. Soc.* 2016; **138**: 499–502.
- Dias LD, Carrilho RMB, Henriques CA, Piccirillo G, Fernandes A, Rossi LM, Ribeiro MF, Calvete MJF and Pereira MM. *J. Porphyrins Phthalocyanines* 2018; **22**: 331–341.
- Groves JT, Nemo TE and Myers RS. *J. Am. Chem. Soc.* 1979; **101**: 1032–1033.
- Kumar D, Tahsini L, de Visser SP, Kang HY, Kim SJ and Nam W. *J. Phys. Chem. A* 2009; **113**: 11713–11722.
- Krest CM, Silakov A, Rittle J, Yosca TH, Onderko EL, Calixto JC and Green MT. *Nat. Chem.* 2015; **7**: 696–702.
- Horowitz S and Trievel RC. *J. Biol. Chem.* 2012; **287**: 41576–41582.
- Shahrokhian S, Seifi H, Bagherzadeh M and Mousavi SR. *Chem. Phys. Chem.* 2004; **5**: 652–660.
- Steiner T and Desiraju GR. *Chem. Commun.* 1998; 891–892.
- Steiner T. *Angew. Chemie, Int. Ed.* 2002; **41**: 48–76.
- Alemohammad T, Safari N, Rayati S, Gheidi M, Mortazavimanesh A and Khavasi H. *Inorg. Chim. Acta* 2015; **434**: 198–208.

23. Mohajer D and Sadeghian L. *J. Mol. Catal. A: Chem.* 2007; **272**: 191–197.
24. Mohajer D, Karimipour G and Bagherzadeh M. *New J. Chem.* 2004; **28**: 740–747.
25. Alemohammad T, Safari N and Osati S. *J. Porphyrins Phthalocyanines* 2011; **15**: 181–187.
26. Aghabali A and Safari N. *J. Porphyrins Phthalocyanines* 2010; **14**: 335–342.
27. Mesbahi E, Safari N and Gheidi M. *J. Porphyrins Phthalocyanines* 2014; **18**: 354–365.
28. Zheng H, Zhang Y, Liu L, Wan W, Guo P, Nyström AM and Zou X. *J. Am. Chem. Soc.* 2016; **138**: 962–968.
29. Liu J, Chen L, Cui H, Zhang J, Zhang L and Su CY. *Chem. Soc. Rev.* 2014; **43**: 6011–6061.
30. Zhang Z, Wojtas L, Eddaoudi M and Zaworotko MJ. *J. Am. Chem. Soc.* 2013; **135**: 5982–5985.
31. Eddaoudi M, Sava DF, Eubank JF, Adil K and Guillerm V. *Chem. Soc. Rev.* 2015; **44**: 228–249.
32. Assen AH, Belmabkhout Y, Adil K, Bhatt PM, Xue DX, Jiang H and Eddaoudi M. *Angew. Chemie, Int. Ed.* 2015; **54**: 14353–14358.
33. Zhang M, Yang Y, Li C, Liu Q, Williams CT and Liang C. *Catal. Sci. Technol.* 2014; **4**: 329–332.
34. Morabito JV, Chou LY, Li Z, Manna CM, Petroff CA, Kyada RJ, Palomba JM, Byers JA and Tsung CK. *J. Am. Chem. Soc.* 2014; **136**: 12540–12543.
35. Horike S, Kadota K, Itakura T, Inukai M and Kitagawa S. *Dalton Trans.* 2015; **44**: 15107–15110.
36. Isimjan TT, Kazemian H, Rohani S and Ray AK. *J. Mater. Chem.* 2010; **20**: 10241–10245.
37. Zhang W, Wang Y, Leng Y, Zhang P, Zhang J and Jiang P. *Catal. Sci. Technol.* 2016; **6**: 5848–5855.
38. Kaur H, Mohanta GC, Gupta V, Kukkar D and Tyagi S. *J. Drug Delivery Sci. Technol.* 2017; **41**: 106–112.
39. Srivastava M, Roy PK and Ramanan A. *RSC Adv.* 2016; **6**: 13426–13432.
40. Shamsaei E, Low Z-X, X. Lin X, Mayahi A, Liu H, Zhang X, Zhe Liu J and Wang H. *Chem. Commun.* 2015; **51**: 11474–11477.
41. Ryder MR, Civalleri B, Bennett TD, Henke S, Rudi S, Cinque G, Fernandez-Alonso F and Tan J-C. *Phys. Rev. Lett.* 2014; **113**: 215502/1–215502/6.
42. Jian M, Liu B, Zhang G, Liu R and Zhang X. *Colloids Surf., A* 2015; **465**: 67–76.
43. Nabipour H, Sadr MH and Bardajee GR. *New J. Chem.* 2017; **41**: 7364–7370.
44. Lu G, Li S, Guo Z, Farha OK, Hauser BG, Qi X, Wang Y, Wang X, Han S, Liu X, DuChene JS, Zhang H, Zhang Q, Chen X, Ma J, Loo SCJ, Wei WD, Yang Y, Hupp JT and Huo F. *Nat. Chem.* 2012; **4**: 310–316.
45. Shringarpure PA and Patel A. *Dalton Trans.* 2010; **39**: 2615–2621.
46. Kumari G, Jayaramulu K, Maji TK and Narayana C. *J. Phys. Chem. A* 2013; **117**: 11006–11012.
47. James AD, Arnold DP and Parsons PG. *Photochem. Photobiol.* 1994; **59**: 441–447.
48. Lindsey JS, Hsu HC and I. C. Schreiman IC. *Tetrahedron Lett.* 1986; **27**: 4969–4970.
49. Adler AL, Long FR and Kampas F. *J. Inorg. Nucl. Chem.* 1970; **32**: 2443–2445.
50. Travis BR, Ciaramitaro BP and Borhan B. *Eur. J. Org. Chem.* 2002: 3429–3434.